PHYSICAL REVIEW A VOLUME 13, NUMBER 5 MAY 1976

Finite-temperature relativistic fluid equations and scaling of high-current beams

G. Ronald Hadley, Thomas P. Wright, and Archie V. Farnsworth, Jr.
Plasma Theory Division, Sandia Laboratories, Albuquerque, New Mexico 87115
(Received 28 October 1975)

Two sets of finite-temperature relativistic fluid equations are obtained by taking moments of the Vlasov equation, using equilibrium and monoenergetic distribution functions. The closed sets of fluid-Maxwell equations are reduced to a simple set of equations under steady-state conditions, using two fluid constants of the motion derived for each set. The set obtained using the monoenergetic distribution is parametrized in cylindrical coordinates for high-current diode studies. The radial scale length for a radial equilibrium superpinch is obtained in terms of macroscopic diode parameters, and radial profiles of the pinch are obtained by solution of the one-dimensional system. It is found that high-current superpinches are characterized by a hot uniform-density core surrounded by a hollow current sheet, and that there is a limit to the current which can be propagated for a given pinch radius, given the macroscopic diode parameters. The minimum pinch radius obtainable in a diode in the steady state is obtained from the hot pinch limit, and diode scaling laws are presented, assuming Child-Langmuir or parapotential flow.

I. INTRODUCTION

In seeking to characterize the behavior of a many-particle system, we are often concerned with determining macroscopic variables such as particle number density, net velocity, current density, pressure, energy flux across a surface, and other quantities which represent some average over a distribution function that describes the phase-space evolution of the system. Many experimental diagnostics allow direct measurement of these or related macroscopic fluid quantities. Solving kinetic systems and obtaining fluid-related information by an appropriate averaging technique is one theoretical method of studying these systems. However, since the kinetic information is lost in the averaging process over momentum space, it is worthwhile trying to obtain a macroscopic description that is consistent with the kinetic system, without having to solve for the kinetic details. We present such an approach here by obtaining fluid equations using physically motivated assumptions on the analytical form of the distribution functions. The specific applications we have in mind are to relativistic electron beams and plasma systems, more generally stated as collisionless Vlasov systems.

We choose specific forms for distribution functions from the general class of three-parameter distributions. The physical meanings of the three parameters are determined by the averages over the distribution which define the particle number density, average velocity vector, and average energy. Depending on the assumed analytical form of the distribution, the whole infinite set of moments may be nonzero, or we may reach some moment which is identically zero. In cases where the fourth and higher moments exist, they are obtained as functions of the first three moments. The advantages of using this approach will become clearer as we consider the nature of fluid equations.

The first three moments of a kinetic equation, such as the Vlasov equation, express conservation of charge (or mass), momentum, and energy. These can be derived for an arbitrary distribution function and are exact.[1] However, they cannot be solved, since they contain more unknown fluid parameters than there are equations. The standard approach is to make certain assumptions on the form of the moments, so that the number of unknowns are reduced to obtain a closed set of fluid equations. The degree of success that solutions to these equations have in describing the macrosscopic behavior of a physical system depend on the shrewdness of the choice leading to closure. The alternative approach which we use is to specify the form of the distribution function *a priori*. For example, consider a collisional system where a choice of a local nonrelativistic Maxwellian distribution for closure leads to the zero-order equations of nonviscous hydrodynamics, whereas the extension of this distribution to a nonlocal one (which depends on spatial gradients as well as local values) leads to the first-order equations of viscous hydrodynamics.[1] In both cases the only parameters entering into the fluid equations are the density, velocity, and temperature, although the latter description is clearly more complete. More generally, by incorporating known physical aspects of a system into a choice of a distribution function, we can incorporate relevant transport properties into the conservation equations.

Nevertheless, since the kinetic system contains more information than the fluid system, situations could arise where the two descriptions would not lead to the same results. For example, collisionless plasmas can exhibit multistreaming of a single species or anomalous transport due to turbulence generated from kinetic instabilities. In such cases the kinetic systems must be studied to obtain the appropriate transport parameters to be included in the fluid analysis. However, the applications which we are principally interested in here (electron beam dynamic behavior in diodes) are situations where we expect that kinetic turbulence and single-species multistreaming effects should be negligible in general. In fact, the steady-state kinetic orbits obtained from particle simulations[2,3] of high-current diodes do not depend on or result from kinetic turbulence.

The two forms of the distribution function which we will consider are monoenergetic and equilibrium.[4] In high-current diodes of interest (MA, MV), the applied voltage is so large that the energy of an electron is principally a function only of its position in the gap (under steady-state conditions). Thus a monoenergetic distribution function incorporates a known kinetic constant of the motion, and should produce fluid equations which describe the macroscopic properties of high-current diodes better than a set obtained from the equilibrium distribution. On the other hand, the fluid equations derived from the equilibrium distribution are expected to have better application to beam-plasma transport problems, where a scattering formalism such as Fokker-Planck can be incorporated.

The derivation of the general time-dependent fluid equations is presented in Sec. II, and they are reduced to steady-state sets in cylindrical geometry in Sec. III. Radial equilibrium flow is examined in Sec. IV, using the equations obtained from the monoenergetic distribution function. A minimum pinch radius r_b is found, and its scaling in terms of diode parameters is given. In Sec. V, we discuss properties of radial flow in pinching diodes to obtain the minimum radius at which purely radial flow can occur. The fluid-Maxwell equations are cast in a dimensionless form in Sec. VI, using scale parameters obtained from the considerations of Secs. IV and V. It is shown here that there is a maximum current density and beam density obtainable in a pinching diode. From the dimensionless parameters which appear in the scaled form of the fluid equations, we are able to argue that the minimum steady-state pinch radius obtainable in a diode is r_b, as obtained in Sec. IV. A necessary condition for a diode to be able to achieve the minimum pinch radius is also established. Solutions to the radial equilibrium equations are obtained in Sec. VII, and profiles of beam density and magnetic field are presented for low- and high-current pinches. Incorporating Child-Langmuir and parapotential flow with the necessary condition for optimum pinching allows us to produce diode scaling for existing and conceptual accelerators in Sec. VIII.

II. DERIVATION OF FLUID EQUATIONS

The relativistic Vlasov equation for electrons can be written

$$\frac{\partial f}{\partial t}+\frac{c\vec{w}}{\gamma}\cdot\frac{\partial f}{\partial \vec{x}}-\frac{e}{mc}\left(\vec{E}+\frac{c\vec{w}}{\gamma}\times\vec{B}\right)\cdot\frac{\partial f}{\partial \vec{w}}=0\,, \tag{1}$$

where c is the speed of light in vacuum, m is the electron rest mass, e is the magnitude of the electronic charge, $\vec{E}$ and $\vec{B}$ are the external and self-consistent electric and magnetic fields, $\vec{w}$ is the dimensionless particle momentum, and $\gamma=(1+w^2)^{1/2}$ is the dimensionless particle energy.

The conservation equations obtained by multiplying Eq. (1) by $1, \vec{w}, \gamma$ and integrating over momentum space are

$$\frac{1}{c}\frac{\partial n}{\partial t}+\nabla\cdot(n\vec{\beta})=0\,, \tag{2}$$

$$\frac{\partial}{\partial t}(n\vec{P})+\nabla\cdot\vec{S}+en(\vec{E}+c\vec{\beta}\times\vec{B})=0\,, \tag{3}$$

$$\frac{1}{c}\frac{\partial \mathcal{E}}{\partial t}+\nabla\cdot(n\vec{P}c)+en\vec{\beta}\cdot\vec{E}=0\,, \tag{4}$$

with the particle number density n, dimensionless fluid velocity $\vec{\beta}$, fluid momentum $\vec{P}$, fluid energy density $\mathcal{E}$, and stress tensor $\vec{S}$ defined by

$$n=\int f\,d^3w\,,\quad n\vec{\beta}=\int\frac{\vec{w}}{\gamma}f\,d^3w,$$

$$n\vec{P}=mc\int\vec{w}f\,d^3w\,,\quad \mathcal{E}=mc^2\int\gamma f\,d^3w,$$

$$\vec{S}=mc^2\int\vec{w}\frac{\vec{w}}{\gamma}f\,d^3w.$$

The conservation equations are exact, and can be generalized to study collisional transport by addition of an appropriate collision term in Eqs. (3) and (4). However, Eqs. (2)–(4) are unsolvable, since they are not closed. In order to obtain a closed set of fluid equations, we approximate f by equilibrium and monoenergetic distribution functions,[4]

$$f_E=[n\xi/4\pi\Gamma K_2(\xi)]\exp[-\xi\Gamma(\gamma-\vec{\beta}\cdot\vec{w})]\,, \tag{5}$$

where $\xi^{-1}=k_B T_R/mc^2$ is the rest-frame temperature (k_B is Boltzmann's constant), $\Gamma=(1-\beta^2)^{-1/2}$, and $K_2(\xi)$ is a modified Bessel function of the second kind of second order with argument ξ; and

$$f_M = \frac{na}{4\pi w_0^2} \frac{\exp(a\vec{\beta}\cdot\vec{w}/\beta w_0)}{\sinh(a)} \delta(w - w_0), \tag{6}$$

with the parameter a determined by the ratio of fluid speed to particle speed,

$$b = \beta\gamma_0/w_0 = \coth(a) - 1/a. \tag{7}$$

It should be noted at this point that we depart from the usual Vlasov equilibrium type of approach,[5-9] since Eqs. (5) and (6) are taken as local distributions whose parameters can be spatially and temporally changing (subject only to macroscopic self-consistency), so that the distributions in general do not identically satisfy the Vlasov equation. Indeed, for the systems we are interested in studying (high-current diodes), not enough kinetic constants of the motion have been determined to obtain, *a priori,* a distribution function which satisfies the Vlasov equation, and kinetic studies have to be performed by computer simulation.[2,3] However, it is unnecessary to impose such a severe restriction on the distribution function to obtain self-consistent macroscopic solutions, since the solutions obtained from the coupled fluid-Maxwell equations are valid macroscopic equilibria for a corresponding Vlasov system. There is an irreversible loss of information in going to the macroscopic description, so that the solutions may be consistent with a whole set of distribution functions. Note that it is not permissible to take the macroscopic solutions alone, and substitute back into the forms of the distribution function given in Eqs. (5) and (6), since they then would imply a specific set of kinetic orbits which may not be the correct ones for the particular system under consideration. In addition to the macroscopic solutions, one needs outside kinetic information to reconstruct the particle orbits. However, we will never have need to do this in this paper, since we are seeking only macroscopic information. Thus by utilizing a more general class of distribution functions than that restricted to satisfying the Vlasov equation identically, we can solve for self-consistent macroscopic equilibria relevant to Vlasov systems.

Proceeding with the development of the fluid equations, we use earlier results[4] for the evaluation of the fluid parameters for the distributions in Eqs. (5) and (6). Using the equilibrium distribution, Eqs. (3) and (4) have the explicit form

$$\frac{1}{c}\frac{\partial}{\partial t}(nF_E\Gamma\vec{\beta}) + \nabla\cdot\left(\frac{n}{\Gamma\xi}\,\vec{1} + nF_E\Gamma\vec{\beta}\vec{\beta}\right) + \frac{en}{mc^2}(\vec{E} + c\vec{\beta}\times\vec{B}) = 0, \tag{3a}$$

$$\frac{1}{c}\frac{\partial}{\partial t}\left(nF_E\Gamma - \frac{n}{\Gamma\xi}\right) + \nabla\cdot(nF_E\Gamma\vec{\beta}) + \frac{en}{mc^2}\vec{\beta}\cdot\vec{E} = 0, \tag{4a}$$

where $F_E = K_3(\xi)/K_2(\xi)$, and $\vec{1}$ is the unit dyad.

For the monoenergetic distribution function we find

$$\frac{1}{c}\frac{\partial}{\partial t}(n\gamma_0\vec{\beta}) + \nabla\cdot\left(\frac{n\beta w_0}{a}\,\vec{1} + nF_M\gamma_0\vec{\beta}\vec{\beta}\right) + \frac{en}{mc^2}(\vec{E} + c\vec{\beta}\times\vec{B}) = 0, \tag{3b}$$

$$\frac{1}{c}\frac{\partial}{\partial t}(n\gamma_0) + \nabla\cdot(n\gamma_0\vec{\beta}) + \frac{en}{mc^2}\vec{\beta}\cdot\vec{E} = 0, \tag{4b}$$

with $F_M = (1 - 3b/a)/b^2$. Equations (2), (3a), and (4a) describe a relativistic ideal gas (isotropic pressure tensor), whereas the monoenergetic set of equations (2), (3b), and (4b) have an essential anisotropy[4] in the pressure tensor. In addition to these equations we need to include Maxwell's equations to compute the self-consistent fields:

$$\nabla\cdot\vec{B} = 0, \tag{8}$$

$$\frac{\partial\vec{B}}{\partial t} + \nabla\times\vec{E} = 0, \tag{9}$$

$$\frac{1}{c^2}\frac{\partial\vec{E}}{\partial t} - \mu_0 cen\vec{\beta}(1 - f_m) - \nabla\times\vec{B} = 0, \tag{10}$$

$$\nabla\cdot\epsilon_0\vec{E} + en(1 - f_e) = 0. \tag{11}$$

In these equations, f_e gives the degree of charge neutralization and f_m gives the degree of current neutralization. The choice of a model for background electron and ion dynamics determines the complexity of these two factors.

III. REDUCTION OF THE STEADY-STATE EQUATIONS

We consider the steady-state behavior of systems which are described by neglecting the time derivatives in the fluid-Maxwell equations

$$\nabla\cdot(n\vec{\beta}) = 0, \tag{12}$$

$$\nabla(n/\Gamma\xi) + n\vec{\beta}\cdot\nabla(F_E\Gamma\vec{\beta}) + (en/mc^2)(\vec{E} + c\vec{\beta}\times\vec{B}) = 0, \tag{13a}$$

$$\nabla(n\beta w_0/a) + n\vec{\beta}\cdot\nabla(F_M\gamma_0\vec{\beta}) + (en/mc^2)(\vec{E} + c\vec{\beta}\times\vec{B}) = 0, \tag{13b}$$

$$\vec{\beta}\cdot\nabla(F_E\Gamma - e\phi/mc^2) = 0, \tag{14a}$$

$$\beta\cdot\nabla(\gamma_0 - e\phi/mc^2) = 0, \tag{14b}$$

$$\nabla\times\vec{B} + \mu_0 cen\vec{\beta}(1 - f_m) = 0, \tag{15}$$

$$\nabla^2\phi = \epsilon_0^{-1} en(1 - f_e), \tag{16}$$

where we have used the steady-state form of Faraday's law to set $\vec{E} = -\nabla\phi$. The set of equations derived from the equilibrium distribution has been used by Toepfer[2,10] to develop a one-dimensional fluid envelope model by introducing further approximations and radially averaging over the two-dimensional cylindrical representation of these equations. However, the steady-state equations may be simplified considerably without introducing any approximations. The fluid equations can be combined to give the equivalent set

$$\frac{\vec{\beta}\vec{\beta}}{\beta^2}\cdot\left(\frac{1}{\Gamma\xi}\nabla\ln Q_E\right)-\vec{\beta}\times\left[\nabla\times(F_E\Gamma\vec{\beta})-\frac{e\vec{B}}{mc^2}+\frac{\vec{\beta}}{\beta^2}\times\left(\frac{1}{\Gamma\xi}\nabla\ln Q_E+\nabla W_E\right)\right]=0\,, \tag{17a}$$

$$\frac{\vec{\beta}\vec{\beta}}{\beta^2}\cdot\left(\frac{\beta w_0}{a}\nabla\ln Q_M\right)-\vec{\beta}\times\left[\nabla\times(F_M\gamma_0\vec{\beta})-\frac{e\vec{B}}{mc}+\frac{\vec{\beta}}{\beta^2}\times\left(\frac{\beta w_0}{a}\nabla\ln Q_M+\nabla W_M\right)\right]=0\,, \tag{17b}$$

$$\vec{\beta}\cdot\nabla W_E=0\,, \tag{18a}$$

$$\vec{\beta}\cdot\nabla W_M=0\,, \tag{18b}$$

with

$$W_E=F_E\Gamma-e\phi/mc^2\,, \tag{19a}$$

$$W_M=\gamma_0-e\phi/mc^2\,, \tag{19b}$$

$$Q_E=[n\xi/\Gamma K_2(\xi)]\,e^{-\xi F_E}\,, \tag{20a}$$

$$Q_M=(na/w_0\gamma_0)\,e^{a/b}/\sinh a\,. \tag{20b}$$

The momentum equations have been separated into two parts, parallel and transverse to the fluid flow. From these equations we see that W and Q are constants of the motion along fluid streamlines for a collisionless system.[11] The constants W_E and Q_E were identified and used in deriving Toepfer's fluid envelope model.[2] The constants W are macroscopic energy constants of the motion, whereas the constants Q can be considered as determining the equation of state for the fluid. In fact, Q_E is a constant of the motion in the general time-dependent problem,[12] and it is the relativistic generalization of the adiabatic ideal-gas law.[2] However, Q_M is only a constant in the steady-state case. Indeed, the monoenergetic assumption itself breaks down for situations where the time variation is too rapid to allow a succession of steady-state solutions.

To further simplify the equations, we consider cylindrically symmetric systems with no azimuthal velocity component. Since we are interested in diode problems, we assume that the fluid streamlines emanate from the cathode surface (or cathode plasma). Since this is an equipotential surface, and fluid elements are born at this surface with the same initial energy, the energy constants W have the same value on all streamlines. Therefore W is a constant everywhere in the diode gap. Similarly, the factor Q is related to the state of the electrons at the cathode plasma (such as density, temperature, etc.) and can be taken as constant everywhere in the diode, since all streamlines intercept the cathode surface.

Thus except for trivial solutions the momentum equations reduce to

$$e\vec{B}/mc=\nabla\times(F_E\Gamma\vec{\beta})\,, \tag{21a}$$

$$e\vec{B}/mc=\nabla\times(F_M\gamma_0\vec{\beta})\,. \tag{21b}$$

The cold-fluid equations used in other work[13] are readily obtained from these equations by taking $\xi=mc^2/k_BT\gg1$ in Eq. (21a) and $a\gg1$ in Eq. (21b), where $\gamma_0=\Gamma$ in the limit. In both cases $F\to1$, and we obtain the cold-fluid expression

$$e\vec{B}/mc^2=\nabla\times(\Gamma\vec{\beta})\,. \tag{21c}$$

For the cold fluid, $W_E\to W_M\to\Gamma-e\phi/mc^2$, and the constants Q_E and Q_M do not enter into the problem.

Finally, we note that ϕ and $\vec{B}$ can be eliminated from the equations to give

$$\nabla^2(F_E\Gamma)=(e^2n/\epsilon_0mc^2)\,(1-f_e)\,, \tag{22a}$$

$$\nabla\times\nabla\times(F_E\Gamma\vec{\beta})=-(e^2n/\epsilon_0mc^2)\,(1-f_m)\vec{\beta}\,, \tag{23a}$$

$$\nabla^2\gamma_0=(e^2n/\epsilon_0mc^2)\,(1-f_e)\,, \tag{22b}$$

$$\nabla\times\nabla\times(F_M\gamma_0\vec{\beta})=-(e^2n/\epsilon_0mc^2)\,(1-f_m)\vec{\beta}\,, \tag{23b}$$

and that by eliminating n from these equations we can obtain a single differential equation for each system whose solution, along with the constants Q and W, give steady-state configurations for specified boundary conditions.

In the remainder of the paper, we will consider only the set of fluid equations obtained from the monoenergetic distribution, since we will be concentrating on physical properties of high-current diodes. The monoenergetic assumption is very good everywhere in the diode gap, except at the cathode emitting surface where the electrons are assumed born with some thermal distribution, and possibly at the anode surface where backscattering from the anode material can introduce an energy spread. We are ignoring the latter effect, and the boundary condition at the cathode just becomes a matching condition to the parameters in the monoenergetic distribution. In this paper we assume that a thermal flux of electrons feeds the cathode emitting surface from a reservoir at temperature T_c, and the parameters in the monoenergetic distribution function are matched to this thermal flux condition at the cathode.

IV. RADIAL EQUILIBRIUM

We now consider the steady-state pinched flow of a relativistic electron beam in a high-current diode, where we expect that the fluid equations derived from f_M should apply. In particular, we address the question of scaling the compressed state of the beam, and subsequently, the structure of the fully pinched beam.

Restricting attention to the tightly pinched region near the anode where space-charge neutrality should hold, we assume conditions of z-independent radial equilibrium, which reduce Eq. (13b) to

$$\frac{dp_\perp}{dr} = ecn\beta_z B_\theta , \tag{24}$$

where[4] $p_\perp = mc^2 n\beta w_0/a$ is the pressure transverse to the beam flow. Ampere's law (15) reduces to

$$\frac{1}{r}\frac{d}{dr}(rB_\theta) + \mu_0 ecn\beta_z = 0 , \tag{25}$$

and the combination of these two equations leads to the pressure balance condition[9]

$$\frac{B_\theta^2(r)}{2\mu_0} = \frac{2}{r^2}\int_0^r p_\perp(r')r'\,dr' - p_\perp(r) . \tag{26}$$

We define the beam radius r_b as that radial position where the kinetic pressure becomes vanishingly small. Solutions of the radial equilibrium equations obtained in Sec. VII give the necessary radial pressure profiles to determine r_b from Eq. (26). However, we can obtain a minimum pinch radius by noting that the high-current pinches ($I > I_A$) are characterized by a uniform density core surrounded by a thin current shell. This configuration gives the highest transverse beam pressure, and hence the smallest beam radius for a given current. Thus the minimum pinch radius is obtained by putting in a step function for p and using the hot-beam ($a \ll 1$) limit,[4] so that Eq. (26) becomes

$$\frac{B_\theta^2(r_b)}{2\mu_0} = \frac{\mu_0 I^2}{8\pi^2 r_b{}^2} = p_\perp(0) = \frac{mc^2 n w_0^2}{3\gamma_0} .$$

Setting $\gamma_0 = \gamma_A$ and $w_0 = w_A$ (values at the anode), we obtain

$$r_b^2 = \frac{3\mu_0 I^2 \gamma_A}{8\pi^2 mc^2 n_A w_A^2} . \tag{27}$$

The number density in the stagnant core, n_A, can be related to the density at the cathode through Eq. (20b), which, in the hot-beam limit, gives $n_c/w_c\gamma_c \approx n_A/w_A\gamma_A$ for a thermal electron flux at the cathode. Assuming that the current density is uniform at the cathode,

$$I = J_c A_c = ecn_c \beta_c A_c , \tag{28}$$

where A_c is the cathode emitting area, and taking thermal flux values for $w_c = (kT_c/mc^2)^{1/2}$ and $\beta_c = (kT_c/2\pi mc^2)^{1/2}$, we obtain the maximum beam compression ratio for a high-current hot pinch from Eq. (27):

$$\frac{\pi r_b^2}{A_c} = \left(\frac{9}{8\pi}\right)^{1/2} \frac{I}{I_A}\left(\frac{w_c}{w_A}\right)^2 , \tag{29}$$

where we have defined an Alfvén-Lawson critical current in terms of the diode voltage $I_A = 4\pi mcw_A/\mu_0 e$. The dependence $r_b \sim I^{1/2}$ clearly shows that the equilibrium propagation of an arbitrarily large current within a fixed radius is not possible. This is an important result of the warm-fluid theory, which says that the density compression is limited by the constant Q, while the random particle energy is limited by the diode voltage. Since this implies a maximum achievable beam pressure, the beam radius must increase as the current increases to maintain the equilibrium pressure balance with the magnetic field. For nominal diode parameters of 2 MV, 10 MA, $kT_c \sim 3$ eV, $A_c \sim 3\times10^3$ cm^2 (appropriate for one side of a high-current double diode), we find $r_b = 1.3$ mm. Since this is essentially the radius used in a previous pellet calculation[14] using even larger currents, we see that it may be necessary to modify present pellet designs to accommodate beam-pinching limits.

V. RADIAL FLOW IN PINCHING BEAMS

In the large-aspect-ratio [(cathode radius)/(diode gap)] diodes of interest for electron-beam-driven fusion implosions, there must be a region of almost purely radial flow for strongly pinching beams. Such a region is characterized by relatively cold flow, $\beta_z \approx 0$, very strong gradients in z, and weak gradients in r. Under these conditions the fluid equations reduce to an r-independent set,

$$\frac{eB}{mc} = \frac{\partial}{\partial z}(F_M \gamma\beta_r) , \tag{30}$$

$$\frac{\partial B}{\partial z} = c\mu_0 en\beta_r , \tag{31}$$

$$\frac{\partial^2\gamma}{\partial z^2} = \frac{e^2}{\epsilon_0 mc^2}(1 - f_e)n , \tag{32}$$

together with the constant of the motion Q_M. Note that since beam self-fields can play an important role in radial flow solutions (the beam space charge bunches the equipotential lines near the anode), the scale length of the z variation, z_0, can be much shorter than the gap spacing ($z_0 \leq d$), where equality holds for the charge-neutral condition $f_e = 1$.

Multiplying Eq. (31) by B, we obtain

$$\frac{d}{dz}\,\frac{B^2}{2\mu_0} = cen\beta_r B$$

or

$$\frac{B^2(r)}{2\mu_0} \leq en_A c \int_0^d \beta_r B\,dz \approx en_A \int_0^d |E_z|\,dz\,, \qquad (33)$$

where we have used the fact that the integrated axial Lorentz force must vanish for radial flow, and that $n \leq n_A$, which is shown in Sec. VI.

This result can be written in the form

$$\mu_0 I^2/8\pi^2 r^2 \leq en_A V\,, \qquad (34)$$

where V is the diode voltage. This expression gives the minimum radius at which purely radial flow can occur:

$$\frac{\pi r_{\min}^2}{A_c} \geq (8\pi)^{-1/2}\,\frac{\gamma_A+1}{\gamma_A}\,\frac{I}{I_A}\left(\frac{w_c}{w_A}\right)^2 \qquad (35)$$

which shows that $r_{\min}$ has essentially the same scaling and is of the same order as the minimum pinch radius r_b given by Eq. (29). This result will be used together with the results of Sec. IV to argue in Sec. VI. that r_b is the minimum pinch radius achievable in a steady-state diode.

VI. SCALING OF THE FLUID EQUATIONS

Guided by the considerations of the previous sections, we normalize the quantities in the fluid equations to order unity in the region of the hot-pinch solution, as discussed in Secs. IV and VII. The cathode parameters which enter into the boundary conditions are the total current I, the cathode area A_c, and the cathode plasma temperature $kT_c \approx mc^2 w_c^2$. The potential is assumed to be zero at the cathode emitting surface and is equal to the gap voltage V at the anode plasma surface. Defining $\gamma_V = 1 + eV/mc^2$,

$$\gamma_A = \gamma_V + (\gamma_c - 1) \approx \gamma_V\,, \qquad (36)$$

where γ_A is the (dimensionless) energy of an electron which was born with $\gamma_c = (1+w_c^2)^{1/2} \approx 1$ and has fallen through the diode potential. Table I lists the physical scales which will be used. The dimensionless set of equations then becomes

$$a_b \frac{\partial}{\partial \tilde{z}}(F_M \tilde{\gamma}\tilde{\beta}_r) - \frac{\partial}{\partial \tilde{r}}(F_M \tilde{\gamma}\tilde{\beta}_z) - 2\frac{I}{I_A}\tilde{B} = 0\,, \qquad (37)$$

$$a_b \frac{\partial \tilde{B}}{\partial \tilde{z}} - 3\frac{I}{I_A}\tilde{n}\tilde{\beta}_r (1-f_m) = 0\,, \qquad (38)$$

$$\frac{1}{\tilde{r}}\frac{\partial}{\partial \tilde{r}}\tilde{r}\tilde{B} + 3\frac{I}{I_A}\tilde{n}\tilde{\beta}_z (1-f_m) = 0\,, \qquad (39)$$

TABLE I. Physical parameters and their scales. Here $n_A = Iw_A\gamma_A(ecA_c\beta_c w_c\gamma_c)^{-1}$ is the maximum beam density obtainable in the diode, as will be seen from the discussion following Eq. (41).

Parameter	r	z	w_0, γ_0	B	$\vec{\beta}$	n
Scale	r_b	$z_0 \leq d$	$w_A \approx w_V$ $\gamma_A \approx \gamma_V$	$\frac{\mu_0 I}{2\pi r_b}$	$\frac{w_A}{\gamma_A}$	n_A

$$a_b^2 \frac{\partial^2 \tilde{\gamma}}{\partial \tilde{z}^2} + \frac{1}{\tilde{r}}\frac{\partial}{\partial \tilde{r}}\left(\tilde{r}\frac{\partial \tilde{\gamma}}{\partial \tilde{r}}\right) - 6\left(\frac{I}{I_A}\right)^2 \tilde{n}(1-f_e) = 0\,, \qquad (40)$$

with $a_b = r_b/z_0 \geq r_b/d$, and

$$\tilde{n} = (\tilde{\gamma}\tilde{w}/b)\,G(a)\,. \qquad (41)$$

The function $G(a) = (b/a)\,e^{3-a/b}\sinh a$ is shown in Fig. 1. It has a maximum value of 0.517 at $a_m = 3.05$. Recall that a cold beam has $a \gg 1$ and a hot beam has $a \ll 1$. The fact that $G(a)/b$ has a maximum at $a = 0$ implies the maximum beam density attainable in the diode is n_A ($\tilde{n} = 1$). This fact, coupled with the energy constant of the motion, implies that there is a maximum beam compression (or pressure) which cannot be exceeded. Also, since $G(a)$ has a maximum, there is a limit to the current density obtainable anywhere in the diode. If the current density at the cathode is J_c, then Eq. (41) implies

$$\frac{J}{J_c} = \frac{G(a)}{G(a_c)}\left(\frac{w}{w_c}\right)^2 \leq 1.4\left(\frac{w_A}{w_c}\right)^2 \approx 1.4\,\frac{eV}{kT_c}\gamma_V\,. \qquad (42)$$

For a 3-MV diode with a cathode plasma temperature of 3 eV, $J < 10^7 J_c$, which gives $J < 10^{10}$ A/cm^2 for a reasonable value of $J_c = 10^3$ A/cm^2.

From Eqs. (37)–(40) we see that there are two dimensionless parameters which characterize the flow. The beam self-magnetic-field is important when the current exceeds the critical current ($I \gtrsim I_A$), although pinching may not occur if the aspect ratio is too large. The parameter a_b gives

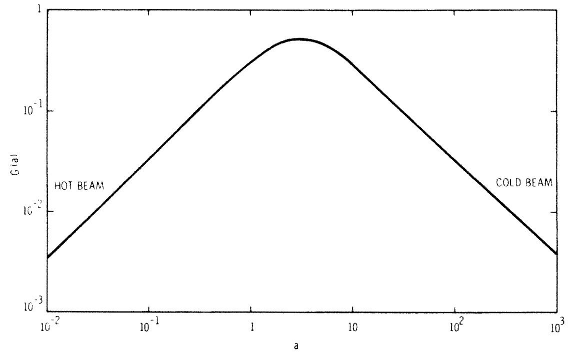

FIG. 1. Isotropy function appearing in current density.

the relative importance of the r and z variation in the flow. For $a_b \ll 1$, the equations reduce to the z-independent set in Sec. IV, which are solved in Sec. VII.

That the hot-pinch radius r_b is the minimum attainable may be seen from considerations of the balance of forces near a minimum in beam radius. For magnetic Lorentz force and kinetic-pressure force balance, the z-independent flow of radius r_b is obtained in Sec. VII. For any other minimum in beam radius, the kinetic-pressure force must exceed the magnetic Lorentz force, resulting in a positive radial acceleration. Under these conditions, Eq. (26) becomes an inequality which leads to $r > r_b$ for any minimum in beam radius other than obtained for z-independent equilibrium.

The scaling used in Eqs. (37)–(40) is such that a sufficient condition for the flow to be pinched to radius r_b can be expressed as $\tilde{r} \sim 1$ (strong pinching occurs in the diode), $I \gg I_A$ (to produce hot stagnant pinch), and $a_b \ll 1$ (neglect z derivatives). In Sec. VII, we solve the radial equations under the last two conditions, and verify that our scaling is correct, so that the beam edge occurs at $\tilde{r} \approx 1$. Now, since $\beta_r \to 0$ at a minimum in the beam radius, and since $a_b \to 0$ as $\beta_r \to 0$ by Eq. (38) (because $\partial \tilde{B}/\partial \tilde{z} \sim 1$), we see that $a_b \ll 1$ is a necessary, but not sufficient, condition that the flow approach the minimum pinch radius r_b. Therefore $r_b \ll z_0 \leq d$ gives us the criterion that a necessary condition for a diode having a planar anode to produce a hot maximally pinched beam which approaches z-independent equilibrium is that the scale factor r_b be much smaller than the gap spacing. Nevertheless, it may be possible to get close to r_b at a local minimum in the two-dimensional flow region without requiring $r_b \ll d$.

VII. SOLUTION OF THE EQUILIBRIUM PINCH EQUATIONS

We assume charge neutralization in the anode plasma ($f_e = 1$), and no current neutralization ($f_m = 0$). For $a_b \ll 1$ and for the current contained within $\tilde{r} \sim 1$, Eqs. (37)–(40) reduce to the one-dimensional set

$$\frac{\partial}{\partial \tilde{r}} (F_M \tilde{\beta}_z) = -2 \frac{I}{I_A} \tilde{B}, \tag{43}$$

$$\frac{1}{\tilde{r}} \frac{\partial}{\partial \tilde{r}} (\tilde{r}\tilde{B}) = -3 \frac{I}{I_A} \tilde{n}\tilde{\beta}_z, \tag{44}$$

$$\tilde{n} = [(\sinh a)/a] e^{3-a/b}, \tag{45}$$

where $\tilde{\gamma} = 1$, $\tilde{w} = 1$. These equations can be solved analytically in the hot ($a \to 0$) and cold ($a \to \infty$) limits, but the transition from hot to cold must be solved numerically. We have obtained solutions to Eqs. (43)–(45) for $r \geq 0$, using boundary conditions specifying $\beta_z(0) = \beta_0$, $B(0) = 0$. Figures 2(a) and 2(b) show solutions for low-current and high-current pinches. The values of current and voltage used in obtaining these solutions were taken from experimental data from pinches obtained on electron beam machines currently in use at Sandia Laboratories.

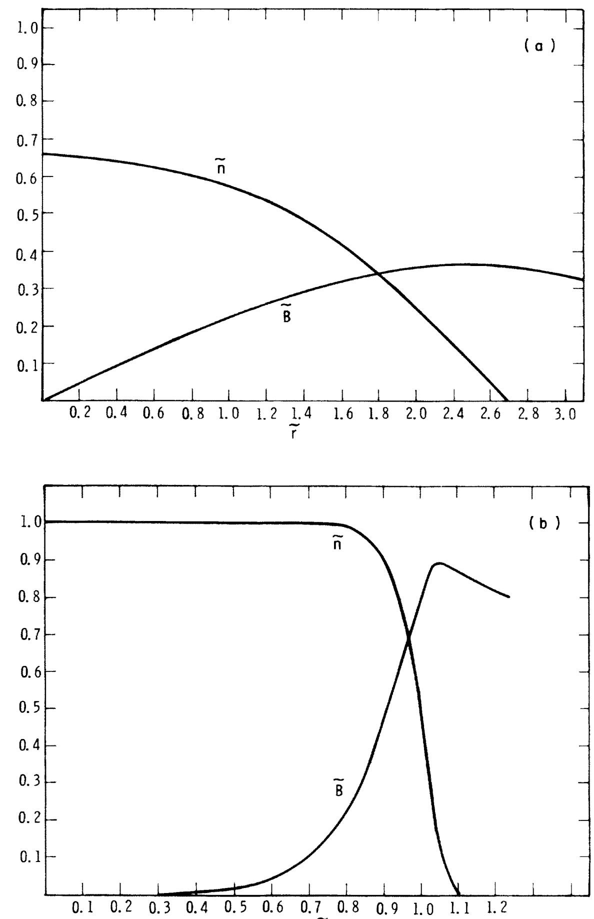

FIG. 2. Solutions to the radial equilibrium equations for (a) $I = 5$ kA, $V = 200$ kV, (b) $I = 108$ kA, $V = 750$ kV.

In the low-current case of Fig. 2(a), we find basically a cold pinch with current and particle densities peaked on axis. For the high-current [Fig. 2(b)] case, however, the equilibrium configuration consists of a region of stagnant flow ($\beta_z \ll 1$) surrounded by a current density shell. Note that the scaling of the beam radius, magnetic field, and density as chosen in Sec. VI is seen to be correct in Fig. 2(b).

The macroscopic equilibria obtained here are consistent with the many axial-current Vlasov models which have been previously constructed,[5-9] especially that of Hammer and Rostoker. These solutions serve as a further justification that our fluid approach gives essentially the same macroscopic results as the corresponding Vlasov solutions. Moreover, our formalism can be readily extended to study cylindrical pinching in diodes, in cases where it is no longer possible to use the Vlasov distribution function approach, because the necessary kinetic constants of the motion are not known *a priori*.

VIII. DIODE SCALING

The parameters which enter into Eqs. (37)–(40) are I/I_A and a_b. We clearly want $I \gg I_A$ for self-magnetic-fields to cause strong pinching in the diode. In particular, we need[15] $I > I_c = I_A R/2d$, where R/d is the diode aspect ratio. The parameter a_b gives the relative importance of the r and z dependence of the flow. Although it is possible to evaluate a_b for a given diode geometry and operating condition, it is worthwhile for scaling purposes to eliminate some of the geometrical aspects by considering two cases where the current and voltage are governed by the Child-Langmuir law,

$$I = 2.34\times 10^3 V^{3/2}(A_c/d^2), \tag{46}$$

and the parapotential[12] law,

$$I = 8500\gamma_V\,(R/d)\ln(\gamma_V + w_V), \tag{47}$$

where the voltage is expressed in MV and current in A. A nonpinching diode should be close to the Child-Langmuir law, whereas a strongly pinching diode may be closer to the parapotential law.

By expressing the cathode area as $A_c = \alpha\pi R^2$, where α depends on the degree of hollowness of the cathode ($\alpha = 1$ for a solid cathode), Eq. (46) gives the diode aspect ratio R/d from the operating load line of a given diode. The parapotential aspect ratio is obtained from the load line by Eq. (47). The operating load line is the current-voltage curve along which a diode can be operated by changing the load impedance. For the Child-Langmuir law, the aspect ratio is

$$R/d \geq 11.7 I^{1/2} V^{-3/4}, \tag{48}$$

where equality holds for $\alpha = 1$, and we have expressed the current in MA and the voltage in MV. The parapotential result is

$$R/d = [118 I/(1+1.96V)] \times\{\ln[1+1.96V+1.98V^{1/2}\,(1+0.978V)^{1/2}]\}^{-1}, \tag{49}$$

with I in MA and V in MV. Equations (48) and (49) can be used to determine the critical current I_c for a given diode, and also can be used with Eq. (29) to determine the value of r_b/d from the diode load line, assuming a value for the cathode plasma temperature. Again using units of MA and MV, and assuming $kT_c \simeq 3$ eV, the Child-Langmuir result is

$$\frac{r_b}{d} = \frac{6.02\times 10^{-2} I}{V^{3/2}(1+0.978V)^{3/4}}, \tag{50}$$

and the parapotential expression is

$$\frac{r_b}{d} = \frac{0.608 I^{3/2}\alpha}{V^{3/4}(1+0.978V)^{3/4}}\;\frac{1}{(1+1.96V)\ln[1+1.96V+1.98V^{1/2}(1+0.978V)^{1/2}]}. \tag{51}$$

By taking the ratio of Eqs. (50) and (48) or Eqs. (51) and (49), the maximum compression ratio can be obtained for the appropriate impedance law. We note that the choice of an effective cathode temperature $T_c \sim 3$ eV is an arbitrary one, and we do not discuss the effect of this parameter in this paper.

The Child-Langmuir scaling is shown in Fig. 3, and the parapotential scaling is shown in Fig. 4, along with the design load lines for one side of several existing and proposed double-diode electron beam machines. As an example of the interpretation of these figures, we discuss Fig. 3. The minimum aspect ratio for a given voltage and diode load line is given in the lower right-hand corner. This determines whether or not the diode will be operating above the critical current for pinching. Three critical current lines have been

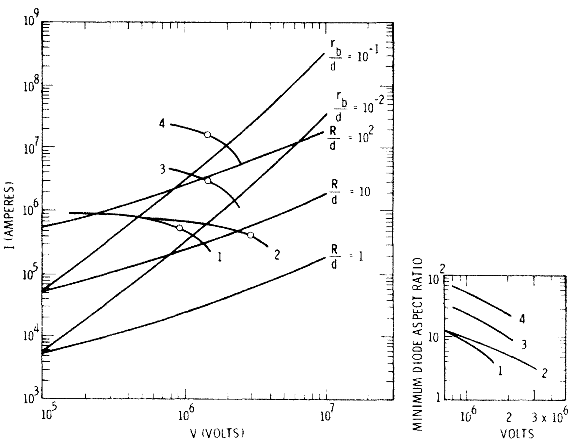

FIG. 3. Diode scaling using Child-Langmuir law. Accelerators (one side): (1) Hydra, (2) Proto-I, (3) Proto-II, (4) conceptual 0.1-Ω matched-load accelerator.

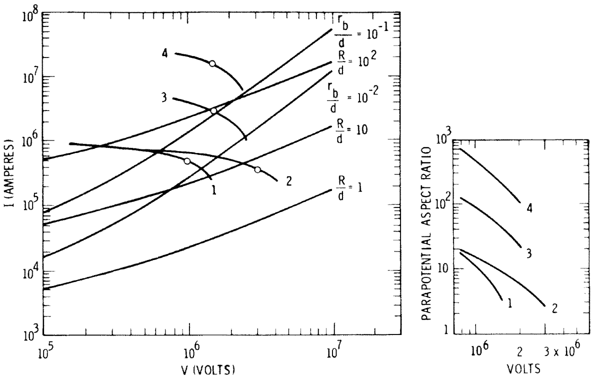

FIG. 4. Diode scaling using parapotential law with accelerators as listed in Fig. 3.

drawn in Fig. 3, labeled by aspect-ratio values of 1, 10, and 100. The load lines indicate what current and voltage the diode will operate at, with the matched load point indicated by a circle. From a point on the load line we obtain the current and voltage to evaluate Eq. (50) and determine the size of r_b/d. Two curves of constant r_b/d are plotted in Fig. 3, for $r_b/d=0.1$ and 0.01. The important result is that an operating point for a given diode must fall far enough above the appropriate critical current line to be able to show appreciable pinching, but it must be below the appropriate r_b/d curve to be able to achieve the minimum pinch radius r_b. The interpretation of the parapotential scaling in Fig. 4 is the same as in Fig. 3. The necessary condition for optimal pinching, $r_b \ll d$, is seen to be more stringent for parapotential scaling than for the Child-Langmuir case.

The conclusion which comes from these figures is that going to higher current at constant voltage not only increases the minimum pinch size (as discussed in Sec. IV), but also makes it increasingly harder for a diode to approach the minimum pinch limit.

IX. CONCLUSIONS

In this paper we have derived sets of finite-temperature relativistic fluid equations for studying macroscopic electron beam behavior, using general equilibrium and monoenergetic distribution functions. The equations have been reduced to a simplified steady-state form, and two fluid constants of the motion have been obtained. The formalism was checked by obtaining solutions to the axial current radial equilibrium problem, and a scaling of hot-beam high-current pinches was obtained which shows that there is a limit to the current which can flow within a given pinch radius.

It has been found that there is a maximum current density obtainable in a diode, and that there is a minimum pinch radius. A necessary condition for a diode to be able to attain the minimum pinch radius r_b has been determined to be $r_b \ll d$, where d is the anode-cathode gap spacing. Parapotential and Child-Langmuir laws have been used to obtain diode scaling information for existing and conceptual accelerators.

ACKNOWLEDGMENT

This work was supported by the United States Energy Research and Development Administration.

[1] K. Huang, *Statistical Mechanics* (Wiley, New York, 1965), Chap. 5.
[2] J. W. Poukey and A. J. Toepfer, Phys. Fluids 17, 1582 (1974).
[3] J. W. Poukey, J. R. Freeman, and G. Yonas, J. Vac. Sci. Technol. 10, 954 (1973).
[4] T. P. Wright and G. R. Hadley, Phys. Rev. A 12, 686 (1975).
[5] D. A. Hammer and N. Rostoker, Phys. Fluids 13, 1831 (1970).
[6] G. Benford and D. L. Book, in *Advances in Plasma Physics*, Vol. 4, edited by A. Simon and W. B. Thompson (Interscience, New York, 1974).
[7] M. E. Rensink, Phys. Fluids 14, 2241 (1971).
[8] J. R. Kan and H. M. Lai, Phys. Fluids 15, 2041 (1972).
[9] P. L. Auer, Phys. Fluids 17, 148 (1974).
[10] A. J. Toepfer, Phys. Rev. A 3, 1444 (1971).
[11] T. P. Wright and G. R. Hadley, Bull. Am. Phys. Soc. 20, 583 (1975).
[12] J. L. Synge, *The Relativistic Gas* (North-Holland, Amsterdam, 1957), Chap. 6.
[13] S. A. Goldstein, R. C. Davidson, J. G. Siambis, and R. Lee, Phys. Rev. Lett. 33, 1471 (1974).
[14] M. J. Clauser, Phys. Rev. Lett. 34, 570 (1975).
[15] J. M. Creedon, J. Appl. Phys. 46, 2946 (1975).